Kidney International, Vol. 67 (2005), pp. 301–313

Equivalence of information from single versus multiple frequency bioimpedance vector analysis in hemodialysis

ANTONIO PICCOLI, GIORDANO PASTORI, MARTA GUIZZO, MIRCA REBESCHINI, AGOSTINO NASO, and CARMELO CASCONE

Department Scienze Mediche e Chirurgiche, University of Padova, Padova, Italy; and Division of Nephrology, University Hospital of Padova, Italy

Equivalence of information from single versus multiple frequency bioimpedance vector analysis in hemodialysis.

Background. In suspended cells, low-frequency current only passes through extracellular fluids, while current at higher frequencies passes through extra- and intracellular fluids. Cells in soft tissues are in contact with each other, which causes tissue anisotropy, meaning that impedance changes along different cell directions, with part of low-frequency current also passing through cells. Hence, equivalent information on body impedance change is expected at all frequencies, which we proved in a dynamic condition of fluid removal with hemodialysis.

Methods. We performed whole-body impedance spectroscopy (496 frequencies from 4 to 1024 kHz, SEAC SFB3 analyzer; Brisbane, Australia) before and during fluid removal (0, 60, 120, 180 min, 2.5 kg) in 67 hemodialysis patients. With increasing current frequency, resistance (R) decreases and reactance (Xc) moves along the Cole's semicircle on the R-Xc plane.

Results. The Cole's semicircles progressively enlarged and moved to the right on the R-Xc plane following fluid removal (increase in both R and Xc values at any given frequency). Xc values at 5 kHz (expected values close to 0 Ohm) were 70% of the maximun Xc, indicating an intracellular current flows at low frequencies. The correlation coefficient between R at 50 kHz (standard frequency) and R at other frequencies ranged from 0.96 to 0.99, and the correlation coefficient between Xc at 50 kHz and Xc at other frequencies at any time point ranged from 0.65 to 0.99.

Conclusion. From high Xc values at low frequency, tissue anisotropy is inferred. Intra- and extracellular current flow causes equivalence of information based on functions of R and Xc measurements made at 50 kHz versus other frequencies.

Bioelectrical impedance analysis (BIA) is a noninvasive method of body composition analysis. Impedance is represented with a complex number (a point) in the real-imaginary plane (Z vector), that is a combination of resistance, R (i.e., the opposition to flow of an alternating current through intra- and extracellular ionic solutions, representing the real part of Z) and reactance, Xc (i.e., the capacitative component of cell membranes and organelles, and tissue interfaces, representing the imaginary part of Z) [1–4].

Key words: bioimpedance, bioimpedance spectroscopy, multifrequency bioimpedance, total body water, intracellular water, extracellular water, hemodialysis, Cole model.

Received for publication October 6, 2003
and in revised form April 29, 2004, and July 1, 2004
Accepted for publication July 14, 2004

© 2005 by the International Society of Nephrology

BIA methods for body composition analysis

Although impedance is an electrical property of tissues that can be directly utilized in body composition analysis, it is commonly embedded in predictive equations that are derived by correlation with criterion measures of body compartments. Literature is divided along 4 methods of body composition analysis based on impedance. The first and the most validated is prediction of total body water (TBW) with functions of 50-kHz single-frequency impedance (either series measures or their parallel equivalents, mostly neglecting the Xc component) [4–9]. The second is prediction of extracellular water (ECW) and TBW with functions of low (1–5 kHz)- and high (100–500 kHz)-frequency impedance (dual- or multiple-frequency BIA), with the intracellular water (ICW) calculated by difference [10–12]. The third is use of many impedance measurements (1 to 1000 kHz) through bioimpedance spectroscopy (BIS) following the Cole's model approach (i.e., extrapolating R values at limit frequencies) for prediction of TBW, ECW, and ICW [13–17] (Figs. 1 and 2). The fourth is use of the direct impedance vector measurement (both R and Xc component) at 50 kHz in a probabilistic graph (vector BIA with the *RXc graph*). Vector BIA is a stand-alone method of body composition analysis, where the continuous, bivariate, random vector of impedance is evaluated through an ordinal scale (tolerance interval percentiles) of the deviation from a reference population. Body composition is then evaluated through patterns of vector distribution with respect to the reference percentiles [18–21].

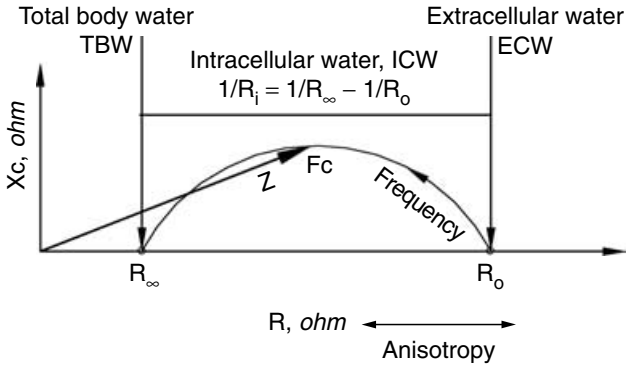

Fig. 1. The semicircle of the Cole's model for cell suspension is utilized in body composition analysis. The curve formed by Z vectors on the R-Xc plane (impedance locus) is a semicircle with a depressed center (see Fig. 2). At the extrapolated zero frequency limit resistance, R_0, current would only flow through the extracellular water solution. The current frequency at which Xc reaches the maximum is the characteristic frequency (Fc). At the extrapolated infinite frequency limit resistance, R_∞, the current would flow through both intra- and extracellular water solution (total body water compartment). The model is not appropriate for human tissues due to their anisotropy (longitudinal conduction of part of low frequency current through muscle cells), which transforms R_0 into a random sum of extra- plus intracellular resistance. R, resistance; Ri, intracellular R; Xc, reactance.

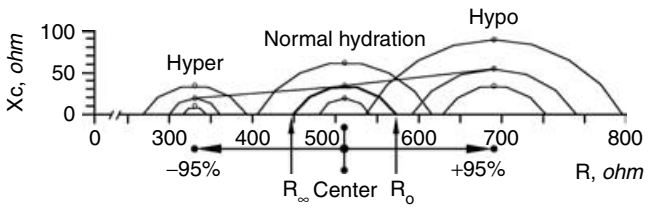

Fig. 2. Effect of between-subject variability of R and Xc on both position and size of an individual Cole's semicircle. In literature, R_0 and R_∞ are derived "without error" from an individual semicircle (e.g., the thick semicircle). Considering independent random errors for both R (horizontal shift of the center, mean R ± 2SD, 95% interval) and Xc component (vertical shift of the center, mean Xc ± 2SD, 95% interval), both circle position and extension dramatically change on the R-Xc plane. Xc at the characteristic frequency (Fc) is represented with an open dot in the vault of each arc. As circles enlarge due to circle migration from left to right, the migration trajectory of individual vectors on the semicircles is linear. Smaller versus larger circles correspond to a more versus less hydrated status as a progressive tissue dehydration increases tissue impedance (real data in Fig. 4). R, resistance; R_0, resistance at 0 frequency; R_∞ at infinity; Xc, reactance.

Errors in BIA and BIS equations

The prediction error of BIA and BIS equations is the sum of 5 errors, namely the impedance measurement error, the regression error (standard error of the estimate against the reference method), the intrinsic error of the reference method (assumptions and measurement error of dilution reference methods and models), the electric-volume model error (anisotropy of tissues and human body geometry other than one cylinder), and the biological variability among subjects (different body composition and body geometry) [3, 9].

In contrast, measurement validity is only required for vector BIA that needs to take care of the measurement error and of the biological variability of subjects [20].

Impedance measurements are made with a 2% to 3% precision error [3, 4, 8, 16, 17]. BIA and BIS equations are validated against dilution methods that have their relevant error, dependent on isotope and compartment, but greater than 3% to 6% [3, 15–17]. For instance, the ratio of ECW/TBW ranged from absurd values of −0.3 to 2.1 following infusion of lactated Ringer's solution [16]. Hence, in addition to costs, low precision prevents clinical utilization of dilution reference methods and models [3, 16, 17].

Although tissue anisotropy (current conduction is not constant in different direction; see Appendix) [1–3, 22] severely impairs validity of BIS in the clinical setting, a panel of BIA experts recommended the utilization of BIS in estimating TBW, ECW, and ICW also in altered fluid distribution. The panel discouraged doctors from using 50 kHz, single-frequency BIA [23].

In this study, using tissue anisotropy as working hypothesis, we wanted to prove that single-frequency 50 kHz-impedance measurements provide the same information as BIS and multifrequency BIA during fluid removal with hemodialysis (HD). To this end, we assessed measurement validity (construct and content validity) of impedance vector at 50-kHz frequency versus other frequencies during fluid removal with HD.

METHODS

Hypothesis

In principle, tissue anisotropy leads to equivalence (meaning similar predictive accuracy) between information provided by single-frequency 50-kHz impedance measurements versus other frequencies, as part of the current at any frequency flows through extra- and intracellular ionic solutions of soft tissues. We tested this hypothesis of equivalence assessing measurement validity (construct and content validity) of BIS versus 50-kHz frequency impedance, considering both steady state and fluid removal with HD (Fig. 2).

Construct validity of BIS (the measurement corresponds to theoretical expectations) was checked by looking at the distribution of Xc at the lowest frequencies, where Xc values were expected both to approach zero (where current flow would only be extracellular), and to be lower than Xc values at the highest frequencies (where impedance becomes progressively independent on cell membrane capacitance). Also, conflicting indications about ICW and ECW changes during dialysis were analyzed.

Content validity (the measurement incorporates the domain of the phenomenon under study) was checked by comparing the amount of information provided by BIS with respect to 50-kHz measurements (correlation

between R and Xc measurements at extreme frequencies versus R and Xc measurements at 50 kHz).

Study design and population

This was a cross-sectional, observational study in maintenance HD patients.

A group of 68 (48 men and 20 women) Caucasian, adult, uremic patients undergoing chronic HD from 6 months or longer (University Hospital in Padua, Italy) gave their informed consent to the study following approval of the local ethical committee. They were treated with thrice weekly, 210 to 240 minutes, standard bicarbonate HD (500 mL/min flow rate, Na 140 mEq/L, K 2 mEq/L, bicarbonate 31 mEq/L, Ca 3.5 mEq/L, Mg 0.7 mEq/L). Natremia at the start of the session was below or above 140 mEq/L in 48 (127 to 140 mEq/L) and 20 patients (140 to 156 mEq/L), respectively. Patients with amputations or metal implants, with cardiac (New York Heart Association class III or higher), pulmonary, or hepatic failure were excluded from the study.

Bioimpedance measurements

Bioimpedance measurements were obtained immediately before (0 min), during the session at 60, 120, 180, 240 minutes, and immediately after the HD session. Whole-body (hand-foot) impedance was measured on ispilateral limbs free from vascular access and following the standard tetrapolar method described elsewhere [4–6]. Adhesive, pregelled electrodes (Q-trace 5400; Kendall-LTP, Chicopee, MA, USA) were not removed from the skin during the dialysis session. Body weight (bed-scale with 50 g sensitivity), blood pressure, and pulse rate were recorded at the same time points. Subjects' height (H) was measured before the session.

In this report we present data collected before the session and at 60, 120, and 180 minutes, which were available in all patients, including those undergoing 210-minute treatments.

Multiple frequency and spectral impedance measurements were obtained with SEAC SFB3 multiple frequency bioimpedance meter (UniQuest-SEAC, Brisbane, Australia) operating with an alternate current of 0.190 mA, and performing measurements on 496 frequencies in the range 4 to 1024 kHz, including a measurement at 50 kHz. Two runs of measurements were performed and recorded for BIS in 30 seconds. The software provided by the manufacturer allowed data transfer to computer, raw data presentation by frequency (R and Xc, or Z magnitude and phase angle at each frequency, including 50 kHz).

Bioimpedance data analysis

BIS and multifrequency BIA. The SEAC software allowed the impedance spectrum fit according to the Cole model (semicircular locus in the R-Xc plane with suppressed center). The impedance semicircle was fitted according to nonlinear least squares fitting procedures (root mean square error of predicted vs. observed Xc, as an indicator of goodness of fit) [14, 15, 24]. One operator (M.G.) performed visual check of goodness of fit of the impedance semicircle through the 496-point vectors recorded at different frequencies in every set of measures. Two runs of 496 frequencies were available in all 68 patients for each of the 4 time points (0, 60, 120, and 180 min) per patient-session, for a total of 544 scattergrams. As the root mean square error criterion utilized by the software is only sensitive to very bad fitting, we ranked goodness of fit according to a 6-point scale based on number and distance of points far from the fitting semicircle: score 5 = very good fit despite up to 3 points far from the fitting circle (75.2% of plots), score 4 = good fit, despite more than 3 points far from the fitting circle (12.4%), score 3 = bad fit at low frequencies (6.6%), score 2 = bad fit at middle frequencies (1.5%), score 1 = bad fit at high frequencies (2.9%), and score 0 = impossible fitting message from software due to high dispersion of vectors at all frequencies around the circle (1.4%). We excluded from statistical analysis 1 patient out of 68, with score 0.

Therefore, we considered 268 semicircles for the statistical analysis, 1 semicircle for each of the 4 time points of the 67 patients (using either the first fitting of the 2 available runs with a comparable score, or the fitting with the higher score).

For the statistical analysis, in addition to the extrapolated, limit R values of BIS, R_o, and R_∞, we also considered the measured vector components R and Xc at 5, 50, 100, 300 kHz, and at the Fc (i.e., the frequency where Xc reaches the maximum) for each of the 268 data sets. R_i was calculated as $1/R_i = 1/R_\infty - 1/R_o$ (see Appendix). Valid Xc values >0 were recorded in the range of frequencies between 5 and 300 kHz (with 2 and 1 exception, respectively), which were considered the lowest and highest frequencies to be utilized for statistical analysis before the limit frequencies of zero and infinity, respectively.

BIS estimates of TBW, ECW, and ICW were provided by the SEAC software according to the Cole and Hanai models, whose equations are described and justified elsewhere [3, 14, 15].

Single frequency BIA at 50 kHz

Conventional BIA. TBW estimate (L) using the impedance measurement at the fixed frequency of 50 kHz was calculated with the sex-specific, regression equations 4 and 5, which have been recently validated (multicomponent model) in a large population by Sun et al, with a SEE of 3.8 (bias 0.5) and 2.6 L (bias 0.3) for healthy males and females, respectively [7]:

$$\text{TBW, in males} = 1.203 + 0.449\ H^2/R + 0.176\ \text{weight} \qquad \text{(Equation 4)}$$

Table 1. Characteristics of hemodialysis patients

	Men $N = 47$		Women $N = 20$		All subjects $N = 67$	
	Mean	SD	Mean	SD	Mean	SD
Age *years*	66.0	13.0	68.0	13.0	67.0	13.0
Dialytic age *years*	2.0	1.9	3.6	9.0	2.5	5.1
Stature *cm*	170.3	7.2	159.7	5.2	167.1	8.3
Average body weight *kg*	71.1	12.2	59.5	9.9	67.6	12.7
Average BMI kg/m^2	24.5	4.2	23.4	4.1	24.2	4.2
Weight loss (60 min) *kg*	0.9	0.3	0.8	0.3	0.9	0.3
Weight loss (120 min) *kg*	1.8	0.5	1.7	0.5	1.7	0.5
Weight loss (180 min) *kg*	2.5	0.7	2.3	1.2	2.5	0.7

$$\text{TBW, in females} = 3.747 + 0.450\ H^2/R + 0.113\ \text{weight} \qquad \text{(Equation 5)}$$

Vector BIA. Bioelectrical impedance vector analysis (BIVA or vector BIA) was performed with the *RXc graph* method [18–20]. An impedance measurement made at 50 kHz is considered a bivariate, normal, random vector with 2 correlated components, R and Xc (a point in the R-Xc plane) [25]. In an *RXc graph*, point vectors are plotted on the reference, sex-specific, bivariate, 50%, 75%, and 95% tolerance intervals of the impedance vector normalized by the subject's height [Z/H = (R/H, Xc/H), in Ohm/m]. These intervals are the ellipses within which the vector of an individual subject falls with a probability of 50%, 75%, and 95%, respectively. We utilized the reference ellipses derived from the healthy Italian population that are available in literature [19].

Statistical methods

The programs of the statistical package BMDP [26] were used for standard calculations, including the Hotelling's T^2 test [25] for mean vector comparison (Program 3D), the repeated-measures analysis of variance (RM-ANOVA, Program 2V), and the linear correlation coefficient *r* (Program 6D). A test *P* level of less than 0.05 was considered as statistically significant.

RESULTS

Characteristics of the 67 HD patients (47 men, and 20 women) are reported in Table 1. One out of the original 68 patients was excluded from statistical analysis because of the impossible fitting of his Cole's arc.

During the first 180 minutes of the HD session, 2.5 kg of fluid was removed (0.9 kg/h during the first and second hour, and 0.7 kg/h during the third hour) (Table 1, Fig. 3).

Vector migration with fluid removal

Parameters of mean impedance vector displacement during the HD session are reported in Table 2.

The average semicircle of the Cole's model progressively enlarged and moved to the right on the R-Xc plane

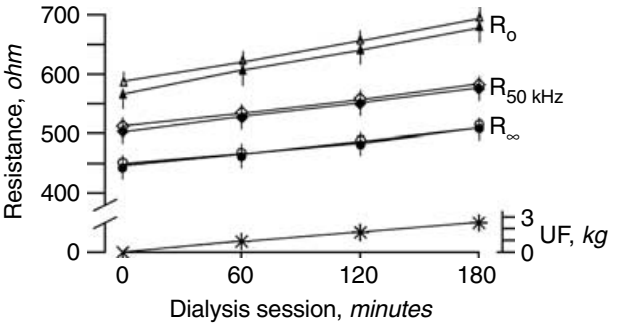

Fig. 3. Mean values of resistance R at limit current frequencies (R_0 and R_∞, at zero and infinity), and at 50 kHz in patients starting the session with natremia below 140 mEq/L (127 to 140 mEq/L, open symbols) or above 140 mEq/L (140 to 156 mEq/L, solid symbols). Variability of R_0, as standard error of the mean (SEM) was 16 and 25 Ohm, SEM of R_∞ was 13 and 21 Ohm, and SEM of R_{50kHz} was 14 and 21 Ohm for low and high natremia, respectively. All mean profiles significantly increased over time ($P < 0.001$, RM-ANOVA) without difference between groups with low versus high natremia. Sodium concentration in dialysis fluid was 140 mEq/L during the entire session for all subjects. Stars shown at the bottom depict fluid removal (ultrafiltration, UF) during the hemodialysis session (SEM 0.5 kg).

(with a progressive downsloping of the negative Xc coordinate of the center) following fluid removal with HD (Tables 2 and 3, Fig. 4). Hence, both R and Xc values progressively increased at any measured frequency. In particular, mean R values, significantly, linearly increased with time both at the limit frequencies, R_o and R_∞, and at 50 kHz (Fig. 3) ($P < 0.001$, RM-ANOVA).

The Fc decreased by 5 kHz (34 to 29 kHz) over 3 hours, indicating a small counterclockwise rotation of impedance spectra with time. As this rotation was associated with increasing circle diameter, the difference between Xc at Fc and at 50 kHz was negligible, between 1.0 and 2.7 Ohm (Table 2, Fig. 4).

There was no significant difference between R profiles over time of patients starting the session with natremia above (140 to 156 mEq/L) versus below 140 mEq/L (127 to 140 mEq/L) (Fig. 3) (RM-ANOVA).

Electric volume change versus fluid removal

In BIS methodology, impedance measurements are transformed by model equations into electric volumes of body fluid compartments, assuming that free fluid in vessels opposes the same impedance as extracellular fluid in tissues (gel fluid). During HD, tissue impedance is also changing over time due to vascular refilling. Nevertheless, following the traditional approach of BIS literature we calculated body fluid volumes during fluid removal as in the steady state before the session.

As a consequence of increasing R_∞ and R_o values, both TBW and ECW significantly decreased with time ($P < 0.001$, RM-ANOVA), either as absolute volume (by 2.38 kg for the TBW, and by 1.98 kg for the ECW)

Table 2. Mean values with standard deviation (SD) of measured impedance vector components at different frequencies, of Cole's semicircle parameters [center, radius, characteristic frequency (Fc)], and of extrapolated R_o, R_∞, and Ri values

	Pre-HD		60 min		120 min		180 min		All time points	
	Mean	SD	Mean	SD	Mean	SD	Mean	SD	Mean	SD
Center, R, Ω	513.0	90.2	535.8	92.8	568.1	95.7	594.7	104.7	553.7	100.5
Center, Xc, Ω	−37.8	11.1	−42.6	15.3	−48.0	15.5	−52.3	15.0	−45.3	15.3
Radius, Ω	76.3	20.1	84.6	25.8	94.3	27.2	102.1	27.3	89.6	27.0
R_o, Ω	579.3	99.5	608.8	104.0	649.2	106.9	682.2	117.9	630.8	113.7
R 5 kHz, Ω	550.9	91.3	578.8	97.7	614.3	100.4	644.2	110.1	597.9	105.7
R 50 kHz, Ω	507.6	88.1	526.8	90.8	554.4	93.1	577.8	100.9	542.3	96.7
R 100 kHz, Ω	487.6	86.2	505.6	89.0	532.2	91.5	554.1	99.0	520.5	94.6
R 300 kHz, Ω	460.7	83.9	477.6	85.5	503.2	89.0	523.1	95.2	491.7	91.2
$R_{\infty,}$ Ω	446.9	83.5	462.8	85.4	487.1	89.1	507.2	95.6	476.6	91.0
Ri, Ω	2065.6	717.2	2059.3	710.5	2090.0	757.1	2100.6	737.1	2079.2	726.9
Xc 5 kHz, Ω	25.6	10.3	29.4	12.1	31.0	12.9	36.1	11.0	30.6	12.2
Xc at Fc, Ω	38.5	9.9	42.0	11.7	46.2	12.9	49.8	13.9	44.2	12.9
Xc 50 kHz, Ω	37.5	9.6	40.5	11.2	44.3	12.1	47.1	12.7	42.4	12.0
Xc 100 kHz, Ω	33.3	7.9	35.5	9.3	38.1	9.9	40.0	10.1	36.8	9.6
Xc 300 kHz, Ω	18.1	5.1	19.1	7.0	20.2	7.9	20.3	7.3	19.5	6.9
Fc, kHz	33.9	6.1	32.1	5.7	30.1	5.2	28.9	7.4	31.2	6.4

Abbreviations are: R, resistance; Ri, intracellular R; Xc, reactance.
R at Fc is the same as Center's R.

Table 3. Mean values with 95% confidence interval (CI) of measured and extrapolated impedance vector components at extreme current frequencies

		Pre-HD	60 min	120 min	180 min	All points
R_o, Ω	Mean	577.3	608.8	649.2	682.2	630.8
	95% CI	554–604	583–634	623–675	653–711	617–645
R 5 kHz, Ω	Mean	550.9	578.8	614.3	644.2	597.9
	95% CI	528–574	555–603	590–639	617–671	585–611
R 300 kHz, Ω	Mean	460.7	477.6	503.2	523.1	491.7
	95% CI	439–482	457–499	481–525	500–546	481–503
$R_{\infty,}$ Ω	Mean	446.9	462.8	487.1	507.2	476.6
	95% CI	423–468	442–484	465–509	484–530	465–488
Xc 5 kHz, Ω	Mean	25.6	29.4	31.0	36.1	30.6
	95% CI	23–28	26–32	28–34	33–39	29–32
Xc at Fc(29–34 kHz), Ω	Mean	38.5	42.0	46.2	49.8	44.2
	95% CI	36–41	39–45	43–49	46–53	43–46
Xc 300 kHz, Ω	Mean	18.1	19.1	20.2	20.3	19.5
	95% CI	17–19	17–21	18–22	19–22	19–20
Xc_{5kHz}: Xc_{300kHz}		1.41	1.54	1.53	1.78	1.57
Xc_{5kHz}: Xc_{Fc}		0.66	0.70	0.67	0.72	0.69

Abbreviations are: R, resistance; Xc, reactance; Fc, characteristic frequency.

or as fractional hydration (1.7% for TBW and 2.5% for ECW, Fig. 5) without significant difference between patients starting the session with natremia above or below 140 mEq/L (Fig. 5).

ICW volume slightly decreased over time (by 0.40 kg, P = ns), following the late increase in Ri after 120 minutes (Table 2). ICW as a fraction of TBW significantly increased with time by 2.5% ($P < 0.001$), without significant difference between patients starting the session with natremia above or below 140 mEq/L (Fig. 5).

The correlation coefficients between TBW, ECW, and ICW changes versus the amount of fluid removal during the session were 0.42 ($P = .001$), 0.58 ($P < .001$), and 0.10 (P = ns), respectively.

The correlation between TBW estimates with BIS versus Sun's formula (R at 50 kHz) was $r = 0.94$ ($P < .001$). The correlation between fluid removal versus change in TBW with Sun's formula was $r = 0.54$ ($P < .001$). Finally, the correlation between TBW changes calculated by BIS versus Sun's formula was $r = 0.71$ ($P < .001$).

Inequalities of Xc values by current frequency

Low frequencies. Xc measurements at 5 kHz were expected to be close to zero due to the postulated, negligible capacitative component of cell membranes (current path only extracellular in the Cole's model) (Figs. 1 and 2). In contrast, Xc values at 5 kHz were not only greater than zero (lower 95% confidence limit higher than 23 Ohm at any time point), but they also were as high as 66% to 73% of the maximun Xc that was reached at the Fc (31 to 34 kHz) (Tables 2 and 3, Fig. 4).

High frequencies. Xc measurements at 5 kHz were expected to be smaller than Xc values at 300 kHz, where the

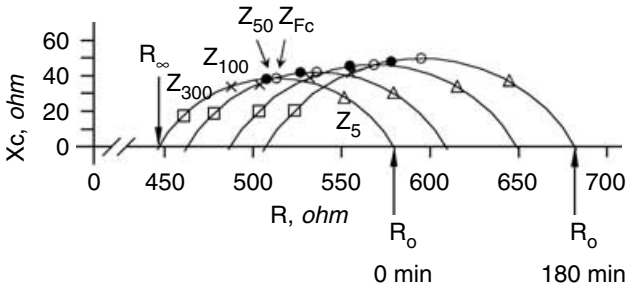

Fig. 4. A Cole's semicircle (mean of all patients) is depicted for every time point of the dialysis session (details in Table 2). As a progressive tissue dehydration increases tissue impedance, circles enlarge and migrate from left to right. The migration trajectory of average vectors with time is linear for each current frequency. Z vectors are indexed by current frequency and represented with different symbols (5 kHz by triangles, Fc by open dots, 50 kHz by solid dots, 100 kHz by ×, and 300 kHz by squares. R, resistance; Xc, reactance; Fc, characteristic frequency.

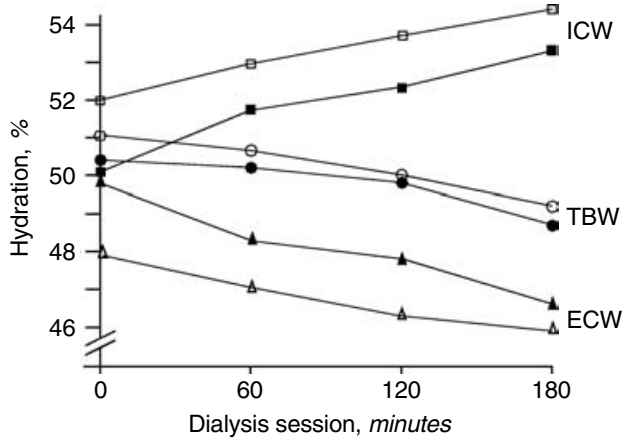

Fig. 5. Mean values of total body water (TBW) as a percentage of the body weight (body hydration fraction), and of both extracellular water (ECW) and intracellular water (ICW) as a percentage of the TBW. TBW and ECW were estimated from R_∞ and R_0, respectively (Fig. 3) according to the Cole's model (see Appendix). Sodium concentration in dialysis fluid was 140 mEq/L during the entire session for all subjects. Patients starting the session with natremia below or above 140 mEq/L are indicated with open and solid symbols, respectively. The change over time in TBW, ECW, and ICW was statistically significant ($P < 0.001$, RM-ANOVA) without a significant difference between groups of natremia (details in the text). Variability of TBW as standard error of the mean (SEM) was 0.95 and 1.4%, and SEM of both ECW and ICW was 0.8% and 1.2% for low and high natremia groups, respectively.

capacitative component of cell membranes is predicted by the Cole's model to be progressively decreasing (Figs. 1 and 2). In contrast, Xc values at 5 kHz were greater than Xc at 300 kHz (by 1.39 to 1.78 times), with a separate 95% confidence interval at any time point (lower 95% confidence limit of 23 Ohm at 5 kHz vs. upper 95% confidence limit of 22 Ohm at 300 kHz; Table 3, Fig. 4).

Therefore, contrary to expectation of the Cole's model, the observed profile of Xc values at 5 kHz indicated a huge contribution of dielectric properties of cells, consistent with tissue anisotropy (i.e., definite contribution of intracellular current flows at low frequencies).

Table 4. Matrix of simple, linear correlation coefficients (r) between impedance vector components, R and Xc, measured at 50 kHz versus other frequencies

	Pre-HD r	60 min r	120 min r	180 min r	All time points r
R 50 kHz versus					
R_o	0.978	0.969	0.964	0.966	0.966
R 5 kHz	0.965	0.982	0.981	0.980	0.980
R at Fc (29–34 kHz)	0.997	0.996	0.995	0.994	0.994
R 100 kHz	0.998	0.998	0.998	0.998	0.998
R 300 kHz	0.995	0.994	0.994	0.994	0.994
R_∞	0.990	0.984	0.983	0.987	0.987
Xc 50 kHz versus					
Xc 5 kHz	0.676	0.740	0.710	0.774	0.774
Xc at Fc (29–34 kHz)	0.995	0.994	0.994	0.994	0.994
Xc 100 kHz	0.987	0.985	0.983	0.982	0.982
Xc 300 kHz	0.781	0.780	0.771	0.649	0.649

Abbreviations are: R, resistance; Xc, reactance; Fc, characteristic frequency.

Inequalities of R values by current frequency

Low frequencies. R measurements at 5 kHz did not significantly differ from R_o, as expected if the current path was only extracellular (Table 3, Figs. 1, 2, and 4).

High frequencies. R measurements at 5 kHz were significantly higher than both R at 300 kHz and R_∞, with separate 95% confidence intervals at any time point. Consistently, the 95% confidence intervals of R_∞ and R at 300 kHz were overlapping at any time point (Table 3, Fig. 4).

Therefore, in agreement with the Cole's model, extreme, measured R values at 5 kHz and 300 kHz matched their limit frequency values of R_o and R_∞, respectively, consistent with different current flow paths at extreme frequencies.

Correlation of impedance at different frequencies

The matrix of simple, linear correlation coefficients (r) between individual vector components, R and Xc, measured at 50 kHz versus components measured at 5 kHz, Fc (31 to 34 kHz), 100 kHz, and 300 kHz is reported in Table 4 and Figures 6 to 10 (Xc values at zero and infinity are zero, by definition).

The correlation coefficient between R at 50 kHz and R at other frequencies ranged from 0.964 ($r^2 = 93\%$, with R_o) to 0.998 ($r^2 = 99.6\%$, with R at 100 kHz) at any time point during the session. Geometrically, as expected by circle properties, there was a clockwise rotation of regression lines from the left to the right of the identity line (regressions with frequencies <Fc lay on the left of the identity line), indicating that different, proportional levels of the same physical phenomenon were measured at different frequencies (Figs. 6 to 8) [27]. In other words, statements on body composition based on functions of R measurements made at 50 kHz are equivalent to those based on other frequencies because they are tightly correlated with each other along straight lines (property of linear transformation of random variables).

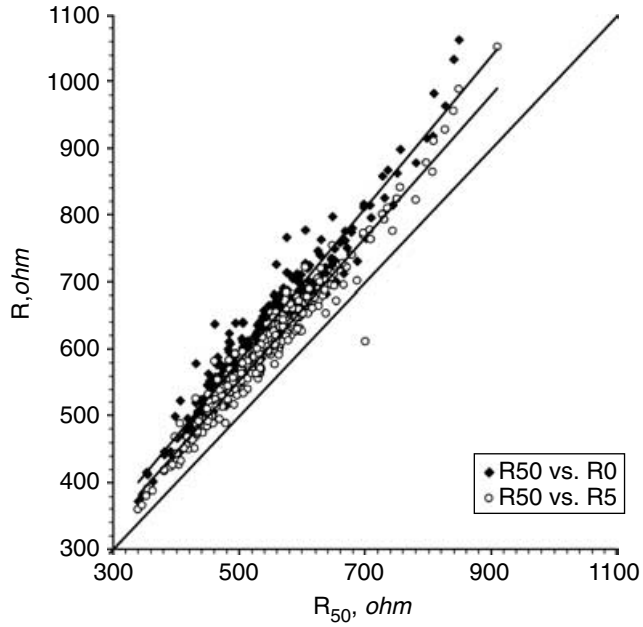

Fig. 6. Scattergram of R values at zero ($r = .97$, $P < .001$, $y = 12.7 + 1.14x$, SEE = 28.1 Ohm) and 5 kHz ($r = .98$, $P < .001$, $y = 18.2 + 1.07x$, SEE = 22.2 Ohm) versus R values at 50 kHz. Both regression lines lie on the left of the identity line.

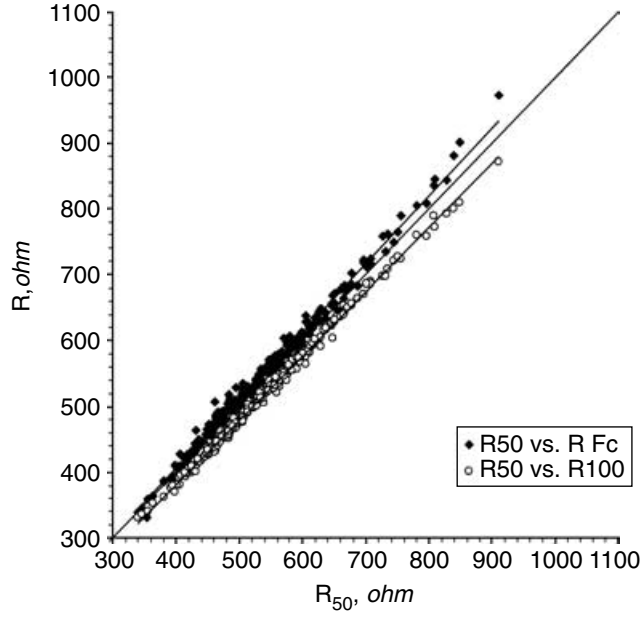

Fig. 7. Scattergram of R values at the characteristic frequency (Fc) ($r = .99$, $P < .001$, $y = -7.2 + 1.03x$, SEE = 9.6 Ohm) and at 100 kHz ($r = .99$, $P < .001$, $y = -9.1 + .98x$, SEE = 5.4 Ohm) versus R values at 50 kHz. The regression lines lie on both the left (R at Fc) and the right (R at 100 kHz) of the identity line.

The correlation coefficient between Xc at 50 kHz and Xc at other frequencies (5 kHz, Fc, 100 kHz, and 300 kHz) ranged from 0.649 ($r^2 = 42\%$) to 0.995 ($r^2 = 99\%$), with a definite gap in the correlation strength between Xc at

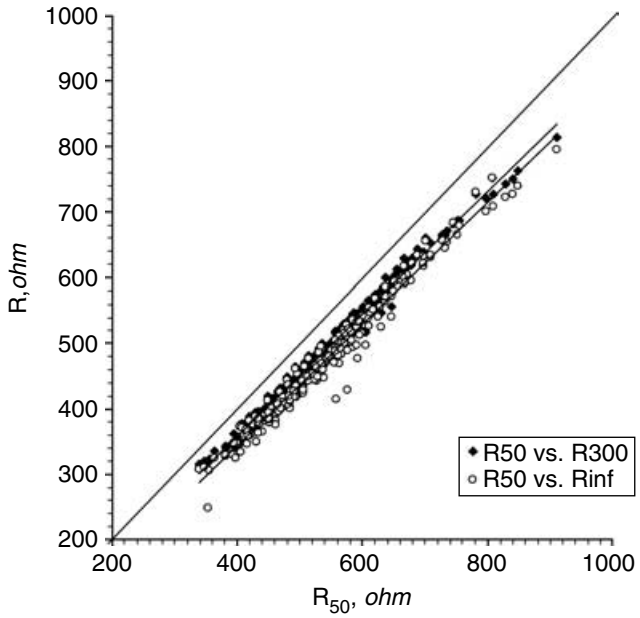

Fig. 8. Scattergram of R values at 300 kHz ($r = .99$, $P < .001$, $y = -17.1 + .94x$, SEE = 9.7 Ohm) and 5 at infinity (Rinf) ($r = .99$, $P < .001$, $y = -27.2 + .93x$, SEE = 14.9 Ohm) versus R values at 50 kHz. Both regression lines lie on the right of the identity line.

50 kHz and Xc at either Fc or 100 kHz ($0.982 < r < 0.995$) versus Xc at either 5 or 300 kHz ($0.649 < r < 0.781$) (Figs. 9 and 10). The moderate correlation with Xc measurements at the extreme frequencies (5 and 300 kHz) might be due to a larger measurement error, to a variable tissue anisotropy effect, or to their combination.

Therefore, statements on body composition based on functions of Xc measurements made at 50 kHz can be considered equivalent to those based on frequencies between Fc (31 to 34 kHz in this population) and 100 kHz.

Overcoming BIS limitations with vector BIA

In BIS methodology, TBW, ECW, and ICW volumes are estimated as deterministic quantities using R_∞, R_o, and Ri values that are derived by extrapolation from the fitting procedure of the Cole's model (Fig. 1). Reference intervals are not available in literature for R_∞, R_o, and Ri at any age. Between-subject variability is considered for the final TBW, ECW, and ICW distributions, which could be utilized with a big prediction error for classification of hydration status into normal or abnormal with respect to norms for TBW, ECW, and ICW. Between-subject variability of these volume estimates includes error sources due to model assumptions, criterion method, and validation equations (Fig. 2) [3, 9, 17]. Factors influencing body composition cause a circle displacement on the R-Xc plane leading to change in the arc extremes, R_∞ and R_o (hence, of Ri), but also of all other vectors at any frequency because their locus is the same circle (Fig. 4).

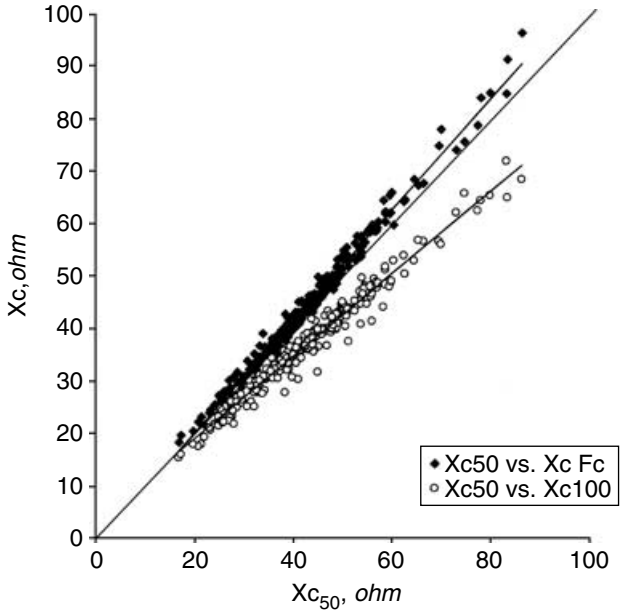

Fig. 9. Scattergram of Xc values at the characteristic frequency (Fc) ($r = .99$, $P < .001$, $y = -1.1 + 1.07x$, SEE = 1.4 Ohm) and 100 kHz ($r = .98$, $P < .001$, $y = 3.2 + .79x$, SEE = 1.7 Ohm) versus Xc values at 50 kHz. The regression lines lie on both the left (Xc) and the right (Xc at 100 kHz) of the identity line.

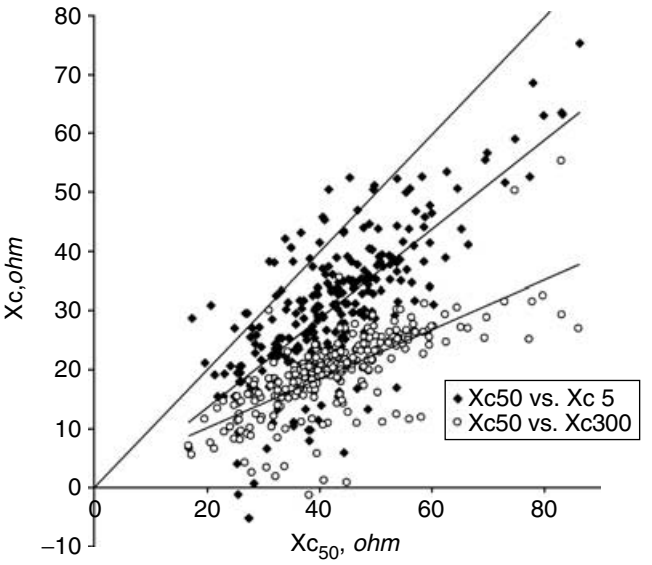

Fig. 10. Scattergram of Xc values at 5 kHz ($r = .75$, $P < .001$, $y = -1.6 + .76x$, SEE = 8.1 Ohm) and 300 kHz ($r = .73$, $P < .001$, $y = 1.5 + .42x$, SEE = 4.7 Ohm) versus Xc values at 50 kHz. Both regression lines lie on the right of the identity line, with Xc values at 5 kHz higher than Xc at 300 kHz (conditional to 50 kHz).

In Figure 11 we transformed the 50 kHz vector from an arc point into a random vector using vector BIA methodology, where an individual, random vector position is compared with both the mean vector position and the between-subject variability of vectors from the reference population (*RXc graph*). The 95%, 75%, and 50% tolerance ellipses (from Italian healthy population [19]) indicate the sex-specific, reference intervals for an individual random vector (normalized by the stature, Z/H in Ohm/m) at 50 kHz. In the figure, dots represent the mean point vectors of dialysis patients (0, 60, 120, 180 min), plotted on their Cole's arc (i.e., the Z_{50} dots in Fig. 4). Compared to male patients, Cole's arcs from women were larger and more translated to the right, although they were normalized by the subject's height. Mean vectors at 50 kHz were longer in women at any time point (Hotelling's T^2 test), but their position in the *RXc graph* followed a same pattern, indicating a comparable hydration status in men and women during the HD session. In either gender, the trajectory of vector displacement was parallel to the major axis of the tolerance ellipses, migrating from between the lower poles of the 50% and 75% ellipses (at 0 min) toward the small axis of ellipses within the median ellipse (at 180 min).

Therefore, we got evidence that in monitoring tissue hydration during fluid removal with HD, no loss of information occurred only considering single-frequency 50 kHz-impedance vector displacement, while no additional valid information was provided by limit frequencies at zero and infinity. Estimates of ECW and ICW provided by BIS equations were apparently artifacts, dependent more on model assumptions and number handling than on information from limit impedance values.

DISCUSSION

Bioimpedance measures have been utilized in body composition analysis since the 1980s in both epidemiologic (population) and clinical (individual) settings. Different BIA approaches aim to transform electrical properties of tissues into clinical information.

In literature, there is discussion about which body compartments can be estimated by BIA methods. Body impedance is generated by the ionic solutions of tissues when an alternate current in the range of 1 to 1000 kHz is injected with available biomedical devices. Most authors agree that at the lowest frequencies, part of the current still passes through cells (i.e., extracellular plus intracellular path), and that at the highest frequencies, part of the current still cannot fully penetrate all cells (i.e., extracellular plus intracellular path) [1–3, 9, 14–17, 22, 23]. The obvious conclusion would be that body impedance specifically reflects the electric volume of intra- and extracellular ionic solutions of tissues (soft tissue hydration status), which can be possibly considered a proxy of TBW volume as determined by dilution reference methods and models. Instead, TBW, ECW, and ICW volumes are estimated, assuming that the current path is only extracellular at the lowest frequencies (negligible intracellular path), and that it is total body at the highest frequencies, with ICW

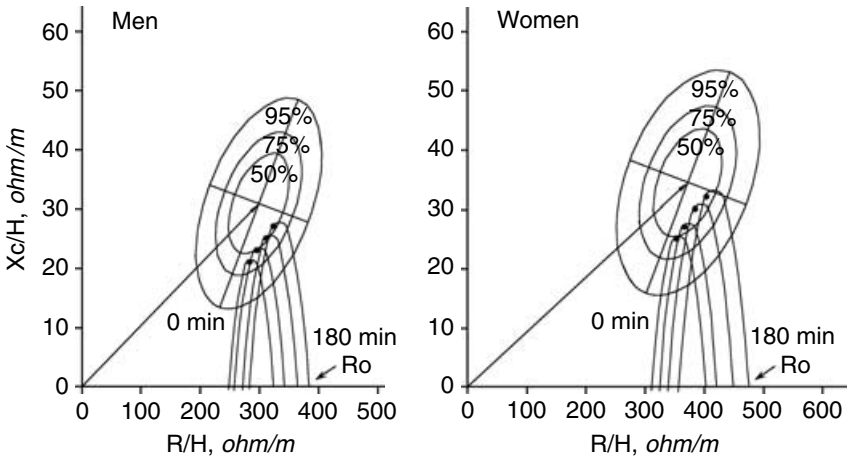

Fig. 11. The 95%, 75%, and 50% tolerance ellipses that are available for the Italian healthy population [19] indicate the sex-specific reference intervals for an individual random vector (normalized by the stature, Z/H in Ohm/m) at 50 kHz, and point vectors represent the mean vectors of dialysis patients, plotted on their hourly Cole's arc (i.e., the Z_{50} dots in Fig. 4). Vectors at 50 kHz are close to the vault of the semicircles where characteristic frequency vectors lie (Z_{Fc}, in Fig. 4) (i.e., the midpoint between R_0 and R_∞). Compared to male patients, Cole's arcs from women were larger and more translated to the right (longer 50 kHz mean vectors at a same time point, as in the healthy population), but their position on the *RXc graph* followed a similar pattern (comparable hydration status) from 0 to 180 minutes, with vector lengthening parallel to the major axis of the tolerance ellipses during fluid removal. Upper and lower poles of the 75% tolerance ellipses represent bioelectric thresholds for dehydration and fluid overload, respectively [20, 40, 44]. In practice, the centripetal property of 50 kHz vectors toward the vault of the corresponding Cole's arc, allows tracking of fluid removal with a direct comparison of impedance with reference intervals of the healthy population.

as the difference between them [10–17, 23]. This point is a matter of assumptions because measurement errors diverge at the extreme frequencies [1, 24, 28]. Nevertheless, in BIS methodology, the extrapolation from measured to the limit, zero, and infinity frequencies is utilized in the hope of overcoming the technical problem. But, as outlined in the Appendix, tissue anisotropy prevents a reliable determination of the extracellular electric volume, which impairs both construct and content validity of BIS methodology.

We wanted to prove that in monitoring tissue hydration during fluid removal with HD, no loss of information occurs, only considering single-frequency, 50 kHz, impedance vector displacement, whereas no additional information is provided by limit frequencies at zero and infinity, and that estimates of ECW and ICW provided by BIS equations are the product of model assumptions and numeric handling of R_o and R_∞.

We recorded the impedance spectrum in 67 patients before and hourly during a HD session, and demonstrated that, following fluid removal, the impedance semicircle progressively enlarged and moved to the right on the R-Xc plane. As a geometric consequence, both R and Xc values progressively increased at any measured frequency, inducing migration of Z vectors along linear trajectories with time (Fig. 4). In particular, mean R values linearly increased with time, both at the limit frequencies, R_o and R_∞, and at 50 kHz (Fig. 3).

Content validity of BIS versus vector BIA

We evaluated content validity of BIS versus single frequency BIA through linear correlation analysis of their impedance measurement distributions. Indeed, a high correlation coefficient (i.e., one measurement can be predicted from the other along any straight line) represents the necessary condition for agreement (meaning interchangeability of measurements from 2 methods, with points lying along the line of equality) [27]. If information from BIS was different from that at 50 kHz, the correlation should have been poor.

The correlation coefficient between R at 50 kHz and R at limit frequencies ranged from 0.964 with R_o to 0.990 with R_∞ at any time point during the session. This means that more than 93% of R variability at limit frequencies could be accounted for by R variability at 50 kHz (Figs. 6 and 8), which means stochastic equivalence (through adaptation of partial regression coefficients) between predictions based on R measurements at 50 kHz and those based on limit frequencies. Similar conclusions were previously reached in smaller samples, and in the steady state of healthy subjects [16, 28] and surgical patients [12, 13].

The correlation between TBW estimates with BIS versus Sun's equation at 50 kHz was high ($r = 0.94$). Moderate correlation coefficients ($0.42 < r < 0.53$) were found between the observed ultrafiltration volume and changes in TBW estimated with either BIS or with Sun's equation. In literature, the correlation between the observed and estimated fluid removal/infusion is moderate with any BIA method [29, 30, 32]. During a HD session, fluid removal from vessels with ultrafiltration is faster than vascular refilling (fluid suction from tissues against a negative interstitial pressure) [31]. The splanchnic and cutaneous blood flow beds have the greatest ability to change their

capacity (80% of the total blood volume) and compensate for fluid removal. The contribution to whole-body impedance is in the order of 10% for the trunk (thorax and abdomen with big vessels) versus 90% of limbs (soft tissue supporting the peripheral vascular refilling) [1, 2]. Therefore, because impedance reflects soft tissue hydration of limbs, which follows intravascular fluid removal with some time delay, only moderate correlations can be found between observed and BIA-estimated fluid removal in the same period of time. Even dilution methods are of no help in acute fluid change [3, 16]. For instance, the change in body weight was used instead of dilution reference methods as criterion method in acute fluid change, since the low precision of diluiton methods would have led to absurd indications (e.g., no increase in TBW, a loss of 0.5 kg ECW, and a loss in ICW following infusion of 2000 mL lactated Ringer's solution) [16].

A greater validity of BIS estimates of TBW and its compartments is postulated (electric models) but not proved in literature, where several results are either of little clinical help or even disappointing [13–15, 23, 29, 30, 32–36]. Indeed, the general accuracy of prediction equation is good with all BIA methods, but without any clinical advantage of BIS compared to either multi-frequency or single-frequency, possibly because the prediction error of equations cannot be lowered [3, 7–17, 23, 28–30, 32–35].

To further demonstrate the equivalence of information from the different BIA approaches, we documented an interesting, centripetal property of 50 kHz vectors with respect to Cole's semicircles. During fluid removal of 2.5 kg, semicircles enlarged, and the Fc decreased from 34 to 29 kHz indicating a little, 5 kHz counterclockwise rotation of impedance spectra with time. The combination of both changes led to a negligible difference between Xc at Fc versus 50 kHz (1.0 to 2.7 Ohm), and between R at Fc (circle center) versus 50 kHz (5 to 17 Ohm) (Figs. 4 and 7). Hence, both center migration and circle enlargement with time can be directly tracked by vector BIA considering both R and Xc vector components at 50 kHz (as *RXc graph*). The tight correlation between Xc values at Fc versus 50 kHz (Fig. 9) supports the extension of the optimal signal-to-noise ratio of Xc measurement made at Fc versus 50 kHz [1]. In BIS, circle enlargement is implicitly utilized in ICW estimation as difference between R_∞ and R_o (Fig. 1).

Construct validity of BIS

Anisotropy is large in soft tissues, particularly in muscles, with a low-frequency conductance ratio of 1:8 between transversal and longitudinal directions [1, 2, 22], which invalidates BIS equations for ECW, and hence, for ICW (Fig. 1) (see Appendix). Anisotropy is considered negligible in BIS literature. If anisotropy was absent or negligible, Xc values at 5 kHz were zero or very small. Instead, during dialysis, mean Xc values at 5 kHz were 66% to 73% of the Xc the Fc (Figs. 4 and 10). The proportion of current flowing through cells at any given frequency depends on Fc that is the frequency at which the effects of cell-membrane capacitance are at a maximum (acting as imperfect capacitors). Xc values at 5 kHz were also greater (1.4 to 1.8 times) than Xc values at 300 kHz, where the capacitative component of cell membranes is progressively decreasing (Figs. 4 and 10). Therefore, contrary to the crucial assumption of the Cole's model, we documented a huge contribution of dielectric properties of cells at 5 kHz frequency, meaning a definite contribution of intracellular current flows at low frequencies (combined EC and IC current path).

These inequalities in Xc values are depicted in figures of several articles, including studies in HD, where focus was on the need for arc extrapolation glossing on validity assessment [14, 15, 24, 28, 37].

The moderate correlation between Xc at 50 kHz and Xc measurements at the extreme frequencies (5 and 300 kHz, Fig. 10) might be due to a larger measurement error (critical signal-to-noise ratio) [1, 24, 28], to a variable tissue anisotropy between subjects, or to their combination.

A further check of construct validity of BIS methodology was obtained by looking at predicted transcellular fluid shift in patients undergoing dialysis with different natremia. Overlapping profiles of R_o and R_∞ over time in patients starting the session with natremia above versus below 140 mEq/L indicated either no transcellular fluid shift or no sensitivity of the method (Fig. 3). BIS model assumptions and numeric handling of R measurements produced a separate, parallel trend in ECW decrease (2% more ECW in hypernatremia) and in ICW increase (2% less ICW in hypernatermia) during the HD session (constant 140 mEq/L Na concentration) (Fig. 5). Even assuming that parallel profiles were split by chance (nonsignificant interaction with time), we found no biological reason for the significant increase in ICW. No change [14, 15], an increase [29, 33], as well as a decrease in ICW [35] after HD have been reported in literature.

Implications for guidelines

A panel of BIA experts recommended the utilization of BIS in estimating TBW, ECW, and ICW also in altered fluid distribution. The panel justified a limited use of 50 kHz, single-frequency BIA, parallel model, in estimating body cell mass, while single-frequency BIA, series model, was ranked as the least useful BIA technique [23]. In contrast, we demonstrated an equivalence of information in fluid monitoring during HD, using measurements at 50 kHz, conventional series circuit, versus BIS with Cole and Hanai model.

Recently, Grimnes and Martinsen [1] published an extensive update of bioimpedance models and techniques

making inconsistent the recommendations of the expert panel and supporting our results, which can be summarized in the following statements: (*1*) electric circuit models do not take into account the difference between an electronic and an ionic medium (biological charge carriers cause relaxation processes, and hence, frequency-dependent capacitance and conductance values); (*2*) when constant-amplitude current is applied to tissues and the corresponding voltage is measured, the raw data and the measured variable are impedance, but the same information can be differently presented as impedance (series circuit models), admittance (parallel circuit models), or as immittance (combined term for impedance and admittance); (*3*) it is impossible to estimate the extracellular electric volume of tissues because an unknown and variable amount of low-frequency current passes through cells (tissue anisotropy), particularly through muscle fibers (parallel direction); (*4*) in BIS, Hanai's and Cole's models (including multiple Cole systems) are only empirical equations that describe impedance changes with current frequency in suspended spherical cells and in several tissues, other than skin, without any correspondence with tissue structure; (*5*) for any combination of electrode position, both the influence of skin impedance and the path of deep current through tissues are frequency dependent. Hence, in BIS, different proportions of tissues and body segments contribute to low and high frequency impedance (unreliable determination of body fluid distribution); (*6*) BIA with a single frequency current (e.g., 50 kHz), close to the characteristic frequency provides the best information at a body level, as it maximizes the signal-to-noise ratio (maximal Xc values in the order of 1/10 of R values), and minimizes both frequency dependent errors and variability of electric flow paths.

Implications in the clinical setting

All equations produce estimates of TBW and of its compartments with a 95% prediction interval too large (±4 to 8 kg, or 2 to 4 kg SEE) for clinical purposes. In principle, segmental impedance measurements might reduce the model error component, but the method cannot be validated with dilution reference methods and models. However, the sum of segment impedance is close to whole-body impedance (0.5% difference) at any frequency, leading either to equivalence of information [28, 30, 38] or to a better prediction of TBW with whole-body impedance [39]. Also, a satisfactory fitting of the Cole's semicircle, either to whole-body or cumbersome segmental measurements, is neither well defined nor always feasible (1 out 68 subjects in this report), which can prevent volume estimation in several cases [33].

Clinical utility of BIA can be achieved following the methodology of elctrocardiogram interpretation, that is, using vector BIA as a stand-alone procedure based on patterns of direct impedance measurements (impedance random vectors) without knowledge of body weight and without a priori assumptions on body composition [18–21]. Using direct measurement and clinical validation of measurement patterns is the only way to bring errors to the minimum because only measurement error and biological variability of subjects are considered [18–21]. Evaluation is in real time (*RXc graph*) at the bedside, based on R and Xc readings at 50 kHz, which are available in a few seconds. After transformation of R and Xc components into bivariate Z scores, the *RXc-score graph* can be used with any analyzer in any population [19].

From clinical validation studies of vector BIA in adults, including HD and peritoneal dialysis patients [40–45], vector displacements parallel to the major axis of tolerance ellipses indicate progressive changes in tissue hydration (dehydration with long vectors, and hyperhydration with short vectors). Consideration of changes of impedance measures, although forfeiting prediction of absolute volumes, allows determination of whether body fluid volumes have returned to those of a reference population group following dialysis, which is not possible with BIS.

From the present results, this pattern proved to be valid in the range of frequencies between 30 and 100 kHz (Figs. 4 and 11), which further documents the robustness of vector BIA.

CONCLUSION

No information was lost when only considering the vector migration at 50 kHz, nor was additional information provided by BIS methodology utilizing either limit frequencies close to zero and infinity (parallel trajectories) or prediction equations of fluid compartments (flawed calculations). The theoretical expectation of vector BIA was that soft tissue hydration change was detectable through impedance measurement at 50 kHz, which has been proved during the HD session (Figs. 3, 4, and 11). In the clinical setting, the comparison of vector position and migration with reference intervals (between-subject variability) represents an additional advantage of vector BIA, which is not allowed with BIS.

APPENDIX

Electric models

Different methods of obtaining body impedance measurements (single or multiple current frequency; distal, proximal, or segmental measures) aim to provide quantitative estimates of body compartments, and are supported by electric models of human body and tissues [1–4, 9]. Complex electrical models are utilized in literature in the hope to increase accuracy, and to reduce prediction error of equations. An electrical model (e.g., series, parallel, Cole's, Hanai's model, etc.) is used as an electrical equivalent [1] that is a circuit that electrically behaves like the original, is expressed through mathematical equations, and aims to

represent anatomic structures or physical processes (e.g., sketches of 75 trillion cells of the human body, 3 to 6 body compartments, cellular and vascular fluid shifts, etc.) [3].

Since the 1950s, the beta-relaxation theory (or Maxwell-Wagner dispersion theory) [1] has been successfully applied to cellular suspension analysis to obtain membrane capacity and intracellular resistivity, allowing accurate measurement of living cell volume by biomass transducers (e.g., industrial fermentation process, blood cell counter). In practice, parameters of the Cole's model are estimated through nonlinear curve fitting in the R-Xc plane of a number of Z vectors that are measured by BIS in a cell suspension [1] (Fig. 1). The curve formed by Z vectors (impedance locus) on the R-Xc plane is a semicircle with a depressed center (Cole's arc, with a negative Xc coordinate) (Fig. 2). At very low frequencies, extrapolated to zero frequency limit, R_o, current only flows through the ECW solution because the cell membrane would act as a capacitor, and the impedance would become ECW resistance. The current frequency at which Xc reaches the maximum is the characteristic frequency (Fc). At very high frequencies, extrapolated to infinite frequency limit, R_∞, the current also penetrates cells such that the impedance becomes TBW resistance. The ICW resistance, R_i, is then derived as $1/R_i = 1/R_\infty - 1/R_o$. ICW and ECW volumes of a suspension containing nonconducting spheres (Hanai's mixture theory) can be estimated introducing in the model 2 constants, which are the resistivity of conducting medium and the concentration of nonconducting spheres [1, 3, 14, 15].

In humans, ECW and ICW volumes are calculated from the extrapolated values of R_o and R_∞, according to Hanai's mixture-volume equation for nonconducting spheres. Three arbitrary constants are needed in the prediction equations, namely, a dimensionless shape factor K_b (4.3 for either gender) accounting for body geometry (arms, legs, and trunk as 5 cylinders), a resistivity constant of the ECW solution k_{ECW} (0.306 in men and 0.316 in women, as a powered ratio of ECW resistivity and body density), and the ratio of ICW/ECW resistivities k_ρ (3.82 in men and 3.40 in women) [15]. As demanded by the model, we used these coefficients as constants in the equations, although they are population specific (by age and gender in healthy subjects) with a very high coefficient of variation, in the order of 19% to 29% [3, 17]. We did not use the correction for time delay of the electric signal, which is recommended for Xitron devices [14, 15], but not for SEAC devices [24].

ECW, ICW, and TBW, in L, were calculated according to equations 1, 2, and 3, respectively [15]:

$$ECW = k_{ECW}/(H^2 \bullet weight^{0.5}/Ro)^{2/3} \quad \text{(Equation 1)}$$

$$(1 + ICW/ECW)^{5/2} = [(Ro + Ri)/Ri] \; [1 + k_\rho \bullet ICW/ECW] \quad \text{(Equation 2)}$$

$$TBW = ECW + ICW \quad \text{(Equation 3)}$$

In literature, the standard error of estimate (SEE, or root mean square error) of TBW, ECW, and ICW prediction equations compared to dilution methods is 1.33 (bias −4.46), 0.90 (bias 2.69), and 1.69 (bias −7.14) L in healthy subjects [15].

Tissue anisotropy invalidates BIS models. Impedance models that work well in suspensions of spherical cells, where Xc is close to 0 Ohm at low frequencies, are flawed in determining intra- and extracellular electrical volumes of cells in tissues because human tissues are anisotropic conductors [1–3, 22]. Anisotropy means that current conduction is not constant in different directions. Anisotropy is small in suspensions of nonspherical cells (e.g., erythrocytes), but is large in tissues because of the orientation of cells, tissue interfaces, macromembranes, and organs, which leads to a progressive increase in Xc values above the expected value of 0 Ohm (only extracellular current path) [1, 22]. Muscle tissue is strongly anisotropic with a low-frequency conductance ratio of 1:8 between transversal and longitudinal directions [1, 2], meaning that a low frequency current (up to 10 kHz) in the longitudinal direction also flows through muscle cells, leading to a biased estimation of the ECW volume (R_o becomes the sum of the extra- plus a variable intracellular R). Lean soft tissues contribute more than fat soft tissues to impedance magnitude because adipocyte droplets (anhydrous triacylglycerols) are poor conductors. Contribution of bone is negligible (meaning nonconductor) in the current range of biomedical analyzers [1–3, 22].

However, as the impedance locus of either whole body or body segments is also an arc, the Cole's model parameters, embedded in Hanai's mixture-volume equation for nonconducting spheres, are utilized in predicting body ECW and ICW volumes of humans (equations 1 to 3) [1, 3, 14, 15].

Correspondence and reprint requests to Prof. Antonio Piccoli, Dpt Scienze Mediche e Chirurgiche, Policlinico IV piano, Via Giustiniani, 2, I-35128 Padova, Italy.
E-mail: apiccoli@unipd.it

REFERENCES

1. Grimnes S, Martinsen ØG: *Bioimpedance and Bioelectricity Basics*, London, Academic Press, 2000
2. Foster KF, Lukaski HC: Whole-body impedance—What does it measure? *Am J Clin Nutr* 64(Suppl):388S–396S, 1996
3. Ellis KJ: Human body composition: In vivo methods. *Physiol Rev* 80:649–680, 2000
4. Kushner RF: Bioelectrical impedance analysis: A review of principles and applications. *J Am Coll Nutr* 11:199–209, 1992
5. Kushner RF, Schoeller DA, Fjeld CR, *et al*: Is the impedance index (ht^2/R) significant in predicting total body water? *Am J Clin Nutr* 56:835–839, 1992
6. Lukaski HC, Bolonchuck WW: Estimation of body fluid volumes using tetrapolar bioelectrical impedance measurements. *Aviat Space Environ Med* 59:1163–1169, 1988
7. Sun SS, Chumlea WC, Heymsfield SB, *et al*: Development of bioelectrical impedance analysis prediction equations for body composition with the use of a multicomponent model for use in epidemiological suerveys. *Am J Clin Nutr* 77:331–340, 2003
8. Houtkooper LB, Lohman TG, Going SB, *et al*: Why bioelectrical impedance analysis should be used for estimating adiposity. *Am J Clin Nutr* 64(Suppl):436S–448S, 1996
9. Heymsfield SB, Wang ZM, Visser M, *et al*: Techniques used in the measurement of body composition: An overview with emphasis on bioelectrical impedance analysis. *Am J Clin Nutr* 64(Suppl):478S–484S, 1996
10. Steijaert M, Deurenberg P, Van Gaal L, De Leeuw I: The use of multi-frequency impedance to determine total body water and extracellular water in obese and lean female individuals. *Int J Obes* 21:930–934, 1997
11. Visser M, Deurenberg P, van Staveren WA: Multi-frequency bioelectrical impedance for assessing total body water and extracellular water in elderly subjects. *Eur J Clin Nutr* 49:256–266, 1995
12. Hannan WJ, Cowen SJ, Fearon KCH, *et al*: Evaluation of multifrequency bio-impedance analysis for the assessment of extracellular and total body water in surgical patients. *Clin Sci* 86:479–485, 1994
13. Hannan WJ, Cowen SJ, Plester CE, *et al*: Comparison of bioimpedance spectroscopy and multi-frequency bio-impedance analysis for the assessment of extracellular and total body water in surgical patients. *Clin Sci* 89:651–658, 1995
14. Matthie J, Zarowitz B, De Lorenzo A, *et al*: Analytic assessment of the various bioimpedance methods used to estimate body water. *J Appl Physiol* 84:1801–1816, 1998
15. De Lorenzo A, Andreoli A, Matthie J, Withers P: Predicting body cell mass with bioimpedance by using theoretical methods: A technology review. *J Appl Physiol* 82:1542–1558, 1997
16. Gudivaka R, Schoeller DA, Kushner RF, Bolt JG: Single- and multifrequency models for bioelectrical impedance analysis of body water compartments. *J Appl Physiol* 87:1087–1096, 1999
17. Ellis KJ, Wong WW: Human hydrometry: Comparison of multifrequency bioelectrical impedance with ^2H_2O and bromine diluition. *J Appl Physiol* 85:1056–1062, 1998
18. Piccoli A, Rossi B, Pillon L, Bucciante G: A new method for monitoring body fluid variation by bioimpedance analysis: The RXc graph. *Kidney Int* 46:534–539, 1994
19. Piccoli A, Nigrelli S, Caberlotto A, *et al*: Bivariate normal values of the bioelectrical impedance vector in adult and elderly populations. *Am J Clin Nutr* 61:269–270, 1995

20. Piccoli A, Pillon L, Dumler F: Impedance vector distribution by sex, race, body mass index, and age in the United States: Standard reference intervals as bivariate Z scores. *Nutrition* 18:153–167, 2002
21. Piccoli A: Patterns of bioelectrical impedance vector analysis: Learning from electrocardiography and forgetting electric circuit models. *Nutrition* 18:520–521, 2002
22. Faes TJC, van der Meij HA, de Munck JC, Heethaar RM: The electric resistivity of human tissues (100 Hz-10 MHz): A meta-analysis of review studies. *Physiol Meas* 20:R1–R10, 1999
23. Ellis KJ, Bell SJ, Chertow GM, *et al*: Bioelectrical impedance methods in clinical research: A follow-up to the NIH technology assessment conference. *Nutrition* 15:874–880, 1999
24. Stroud DB, Cornish BH, Thomas BJ, Ward LC: The use of Cole-Cole plots to compare two multi-frequency bioimpedance instruments. *Clin Nutr* 14:307–311, 1995
25. Jolicouer P: *Introduction to Biometry*, New York, Kluwer Academic/Plenum Publishers, 1999
26. Dixon WJ, Brown MB, Engelman L, Jennrich RI: BMDP statistical software manual, Berkeley, UCLA, 1992
27. Bland JM, Altman DG: Statistical methods for assessing agreement between two methods of clinical measurement. *Lancet* i:307–310, 1986
28. Van Marken Lichtenbelt W, Westerterp KR, Wouters L, Luijendijk SCM: Validation of bioelectrical-impedance measurements as a method to stimate body-water compartments. *Am J Clin Nutr* 60:159–166, 1994
29. Cox-Reijven PL, Kooman JP, Soeters PB, *et al*: Role of bioimpedance spectroscopy in assessment of body water compartments in hemodialysis patients. *Am J Kidney Dis* 38:832–838, 2001
30. Chanchairujira T, Metha RL: Assessing fluid change in hemodialysis: Whole body versus sum of segmental bioimpedance spectroscopy. *Kidney Int* 60:2337–2342, 2001
31. Guyton AC: *Textbook of Medical Physiology*, 8th ed., Philadelphia, Saunders, 1991, pp 282
32. O'Brien C, Baker-Fulco CJ, Young AJ, Sawka MN: Bioimpedance assessment of hypohydration. *Med Sci Sports Exerc* 31:1466–1474, 1999
33. Jaffrin MY, Fenech M, De Fremont JF, Tolani M: Continuous monitoring of plasma, interstitial, and intracellular fluid volumes in dialyzed patients by bioimpedance and hematocrit measurements. *ASAIO J* 48:326–333, 2002
34. Patel RV, Peterson EL, Silverman N, Zarowitz BJ: Estimation of total body and extracellular water in post-coronary artery bypass graft surgical patients using single and multiple frequency bioimpedance. *Crit Care Med* 24:1824–1828, 1996
35. Spiegel DM, Bashir K, Fisch B: Bioimpedance resistance ratios for the evaluation of dry weight in hemodialysis. *Clin Nephrol* 53:108–114, 2000
36. Scharfetter H, Monif M, Laslo Z, *et al*: Effect of postural changes on the reliability of volume estimations from bioimpedance spectroscopy data. *Kidney Int* 51:1078–1087, 1997
37. Dewit O, Ward L, Middleton SJ, *et al*: Multiple frequency bioimpedance: A bed-side technique for assessment of fluid shift patterns in a patient with severe dehydration. *Clin Nutr* 16:189–192, 1997
38. Zhu F, Schneditz D, Levin NW: Sum of segmental bioimpedance analysis during ultrafiltration and hemodialysis reduces sensitivity to changes in body position. *Kidney Int* 56:692–699, 1999
39. Deurenberg P, Deurenberg-Yap M, Schouten FJM: Validity of total and segmental impedance measurements for prediction of total body composition across ethnic population groups. *Eur J Clin Nutr* 56:214–220, 2002
40. Piccoli A, for the Italian HD-BIA Study Group: Identification of operational clues to dry weight prescription in hemodialysis using bioimpedance vector analysis. *Kidney Int* 53:1036–1043,1998.
41. Piccoli A, Brunani A, Savia G, *et al*: Discriminating between body fat and fluid changes in the obese adult using bioimpedance vector analysis. *Int J Obesity* 22:97–104, 1998
42. Piccoli A, Pittoni G, Facco E, Pillon L: Relationship between central venous pressure and bioimpedance vector analysis in critically ill patients. *Crit Care Med* 2000; 28:132
43. Guglielmi FW, Mastronuzzi T, Pietrini L, *et al*: The RXc graph in evaluating and monitoring fluid balance in patients with liver cirrhosis. *Ann N Y Acad Sci* 873:105–111, 1999
44. Piccoli A, for the Italian CAPD-BIA Study Group: Bioelectrical impedance vector distribution in peritoneal dialysis patients with different hydration status. *Kidney Int* 65:1050–1063, 2004
45. Pillon L, Piccoli A, Lowrie EG, *et al*: Vector length as a proxy for the adequacy of ultrafiltration in hemodialysis. *Kidney Int* 66:1266–1271, 2004